

Modeling Self-Propagating Malware with Epidemiological Models

Alesia Chernikova* Nicoló Gozzi† Simona Boboila* Nicola Perra‡ Tina Eliassi-Rad* Alina Oprea*

*Northeastern University †University of Greenwich ‡ School of Mathematical Sciences, Queen Mary University of London

Abstract—Self-propagating malware (SPM) has recently resulted in large financial losses and high social impact, with well-known campaigns such as WannaCry and Colonial Pipeline being able to propagate rapidly on the Internet and cause service disruptions. To date, the propagation behavior of SPM is still not well understood, resulting in the difficulty of defending against these cyber threats. To address this gap, in this paper we perform a comprehensive analysis of a newly proposed epidemiological model for SPM propagation, *Susceptible-Infected-Dormant-Recovered* (SIIDR) [5]. We perform a theoretical analysis of the stability of the SIIDR model and derive its basic reproduction number by representing it as a system of Ordinary Differential Equations with continuous time. We obtain access to 15 WannaCry attack traces generated under various conditions, derive the model’s transition rates, and show that SIIDR fits best the real data. We find that the SIIDR model outperforms more established compartmental models from epidemiology, such as SI, SIS, and SIR, at modeling SPM propagation.

I. INTRODUCTION

Self-propagating malware (SPM) is one of today’s most important security threats that has resulted in huge financial losses and data breaches with high economic and social impacts. For instance, the notorious WannaCry [22] attack first discovered in 2017 and still actively used by attackers today was estimated to have affected more than 200,000 computers across 150 countries, with total damages ranging from hundreds of millions to billions of dollars. In May 2021, the Colonial Pipeline [36] cyber-attack caused the shut down of the entirety of the Colonial gasoline pipeline system for several days. It affected consumers and airlines along the East Coast of the United States and was deemed a national security threat. Another infamous worldwide SPM attack is Petya [37], first discovered in 2016 when it started spreading through phishing emails. Petya represents a family of various types of ransomware responsible for estimated damages of over 10 million dollars. Given the present cyber-crime landscape with new threats emerging daily, it becomes significantly important to be able to model SPM behavior. A deep understanding of self-propagating malware characteristics gives us an opportunity to identify similar threats, define control strategies, and design proactive defenses against these attacks. A large body of research has looked into designing methods to detect and remove malware [28], but less so in finding best models that capture its behavior. The majority of existing works on SPM modeling focus on theoretical analyses of infection spreading [12], [14], [20], [26], lacking a thorough real-world evaluation of these models.

In this paper, we model the behavior of a well-known

SPM attack, WannaCry, based on real-world attack traces. The similarities between the behavior of biological and computer viruses enable us to leverage compartmental models from epidemiology. We adopt a novel compartmental model called SIIDR [5], and conduct a thorough analysis to show that SIIDR is capable of accurately modeling WannaCry dynamics. Additionally, we derive the infection-spreading rates that characterize actual WannaCry attacks.

Epidemiological models divide a population into compartments describing the various stages of an illness. Their number and characteristics depend on the disease under study. Following the natural history of the disease, individuals transition from one compartment to another either spontaneously (e.g., recovery process) or after interactions (e.g., infection process) at given rates that depend on the characteristics of the disease. Prototypical models, that act as building blocks for many others, are the SI, SIS and SIR models [4], [16]. SI models are used to describe diseases where infection is permanent. They feature two compartments and one transition. The susceptible compartment S represents healthy individuals that interacting with infectious individuals in the compartment I might get infected. SIS models feature two compartments as well, but two transitions. Beside the infection process as in the previous model, we have a recovery process: infected individuals spontaneously recover and become susceptible to disease again. Hence, they are used to model diseases that can infect us multiple times. SIR models instead, capture diseases from which we develop a permanent immunity. They feature three compartments and two transitions. Infected individuals that are no longer infectious join the recovered compartment R .

In their simplest incarnation epidemic models are represented by a system of Ordinary Differential Equations (ODEs) under a homogeneous mixing approximation that assumes a well mixed population where everyone is potentially in contact [35]. We demonstrate that classic models are not sufficient to accurately describe self-propagating malware. In particular, the investigation of real WannaCry attacks showed that consecutive infection attempts originating from the same host are delayed by a variable time interval. These findings prompted us to study SIIDR: a model that features a new state, Infected Dormant (I_D), along with the S , I , R compartments. During the dormant state, an infected host temporarily ceases to pass infection to its neighbors, until it transitions back to the Infectious state.

In this work, we present a comprehensive analysis of SIIDR. We study the model assuming a well mixed pop-

Notation	Meaning
S	Number of Susceptible Individuals
I	Number of Infected Individuals
I_D	Number of Infected Dormant Individuals
R	Number of Recovered Individuals
SPM	Self-Propagating Malware
ODE	Ordinary Differential Equation
AIC	Akaike Information Criterion
ABC	Approximate Bayesian Computation
ABC-SMC (SMC)	Sequential Monte-Carlo Approach
ABC-SMC-MNN (SMC)	Sequential Monte Approach when Covariance Matrix is Calculated using M Nearest Neighbors of the Particle
SI	Susceptible-Infected Compartmental Model
SIS	Susceptible-Infected-Susceptible Compartmental Model
SIR	Susceptible-Infected-Recovered Compartmental Model
SIIDR	Susceptible-Infected-Infected Dormant-Recovered Compartmental Model
β	Infection Rate
$\bar{\beta}$	Infection Probability
μ	Recovery Rate
γ_1	Transition Rate from Infected to Infected Dormant Compartment
γ_2	Transition Rate from Infected Dormant to Infected Compartment
R_0	The Basic Reproduction Number
G	Next-generation Matrix
E^*	Equilibrium Point for SIIDR Represented as the System of ODEs

Table I: Terminology and abbreviations used in the paper.

ulation of hosts and derive the basic reproduction number R_0 – a fundamental epidemic concept that characterizes the transmission potential of a disease [8], [17], [34]. R_0 is the number of secondary cases generated by an infectious seed in a fully susceptible population. It describes the epidemic threshold, thus the conditions necessary for a macroscopic outbreak ($R_0 > 1$) [10], [34]. We also investigate equilibrium or fixed points of SIIDR as they provide insights on how to contain or suppress the spreading of malware.

We reconstruct the dynamics of WannaCry from real traffic logs and use the Akaike Information Criterion (AIC) [2] to demonstrate that SIIDR captures the malware behavior better than classical epidemic models such as SI, SIS, SIR. Further, we determine the transition rates that characterize the WannaCry propagation, using Sequential Monte-Carlo technique. We believe that the research community can greatly benefit from reconstruction-based modeling of actual attacks, a challenging task that we undertake in this paper. The SIIDR model and corresponding transition rates can be used as the basis for future studies that enable validation of defensive techniques through realistic SPM simulations.

To summarize, our contributions are the following:

- We reconstruct the SPM dynamics using real-world WannaCry traces that were obtained by running a vulnerable version of Windows in a virtual environment.
- We analyze an epidemic model called SIIDR [5] and demonstrate that it captures the behavior of WannaCry traces.
- We derive the basic reproduction number of SIIDR and discuss the stability conditions of its associated system of ODEs for networks operating under the homogeneous mixing assumption.
- We show that SIIDR outperforms several classical models in terms of capturing WannaCry behavior, and derive the model’s transition rates from actual attacks.

We organize the rest of the paper as follows: in Section II we provide background information about the WannaCry

malware and the most common compartmental models of epidemiology. We also define the threat model and problem statement. In Section III we introduce SIIDR, discuss the derivation of R_0 and the stability of the model. Section IV presents the methodology for model selection and estimation of transition rates. In addition, Section V presents the experimental results that support the findings of the paper. We conclude in Section VII. Table I includes common terminology used in the paper.

II. BACKGROUND AND PROBLEM STATEMENT

A. WannaCry Malware

WannaCry is a self-propagating malware attack, which targets computers running the Microsoft Windows operating system by encrypting data and demanding ransom in Bitcoin cryptocurrency. It automatically spreads through the network and scans for vulnerable systems, using the EternalBlue exploit to gain access, and the DoublePulsar backdoor tool to install and execute a copy of itself. WannaCry malware has a ‘kill-switch’ that appears to work like this: part of WannaCry’s infection routine involves sending a request that checks for a web domain. If its request returns showing that the domain is alive or online, it will activate the ‘kill-switch’, prompting WannaCry to exit the system and no longer proceed with its propagation and encryption routines. Otherwise, if the malicious program can not connect to the domain, it encrypts the computer’s data, then attempts to exploit the SMB vulnerability to spread out to random computers on the Internet, and laterally to computers on the same network [38].

B. Epidemiological Models

Compartmental models are mathematical techniques to describe infectious diseases. The most common examples are SI, SIS, and SIR models. One way to represent the dynamics of these models is to use a system of ODEs with continuous time. In their simplest form, they assume a homogeneous mixing, that is, every node is potentially in contact with all the others.

1) *SI model*: The SI model has the following dynamics:

$$\frac{dS}{dt} = -\beta S \frac{I}{N} \quad (1)$$

$$\frac{dI}{dt} = \beta S \frac{I}{N}, \quad (2)$$

(3)

Due to the homogeneous mixing assumption, the per capita rate at which susceptible individuals get infected is given by the probability of interacting with an infected individual (I/N) times the transmission rate of the disease β . The state diagram for SI is represented in Figure 1.

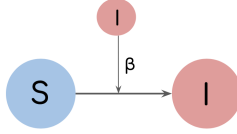


Figure 1: Transition diagram for one node n_i at some time step t corresponding to SI model.

2) *SIS model*: The SIS model can be represented as follows:

$$\frac{dS}{dt} = -\beta S \frac{I}{N} + \mu I \quad (4)$$

$$\frac{dI}{dt} = \beta S \frac{I}{N} - \mu I, \quad (5)$$

(6)

where μ is recovery rate of the disease. Note how the recovery process is spontaneous and does not require any interaction. Hence, each infected individual, has an average duration of infection of μ^{-1} . The state diagram for SIS is shown in Figure 2.

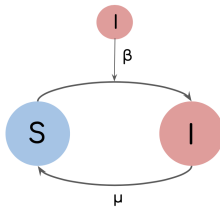


Figure 2: Transition diagram for one node n_i at some time step t corresponding to SIS model.

3) *SIR model*: The system of differential equations corresponding to SIR model is the following:

$$\frac{dS}{dt} = -\beta S \frac{I}{N} \quad (7)$$

$$\frac{dI}{dt} = \beta S \frac{I}{N} - \mu I \quad (8)$$

$$\frac{dR}{dt} = \mu I, \quad (9)$$

where as above β is the infection rate, and μ is recovery rate. The state diagram for SIR is represented in Figure 3.

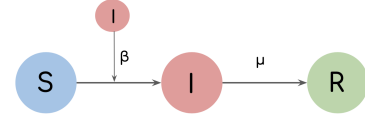


Figure 3: Transition diagram for one node n_i at some time step t corresponding to SIR model.

C. Problem Statement and Threat Model

We aim to understand and capture the behavior of one of the most devastating cyber-threats today, self-propagating malware. The objective of our work is to provide a rigorous mathematical analysis of realistic SPM attacks, and thus lay down the foundation of efficient defense strategies against these prevalent threats. Several works propose models to capture the behavior of SPM [12], [14], [20], [26], however, the vast majority of them have only theoretical analysis and do not incorporate the information about real-world SPM traces. Thus, they lack the proof that the introduced models apply to real-world scenarios. Additionally, it is hard to perform comparative analyses to other models in these settings. Existing work that uses real-world data for modeling SPM [19] leverages basic models of epidemiology with the small number of possible compartments, thus, is not enough to capture more comprehensive characteristics of malware. To this end, we are using a more advanced model of epidemiology (SIIDR) to derive the characteristics of a well-known malware, WannaCry, using real-world attack traces.

In addition to determining which epidemiological model fits best real WannaCry attack traces, our second goal is to infer the parameters of the SIIDR epidemic model for different malware variants. Parameter inference is crucial for enabling attack simulations on real networks to measure the impact of the attack, as well as the effectiveness of defensive measures. Once the parameters of the attack are known, an analyst can compute the basic reproduction number of the attack, and understand whether the attack will result in an epidemic. In the case of computer networks represented as graphs, a defender might configure its network topology by performing edge or node hardening [18], [30], [32], minimizing the leading eigenvalue of the graph to prevent the damage from self-propagating malware attacks, or using anomaly detection methods to detect the malware propagation [28].

Our goal is to model SPM propagation inside a local network (such as an enterprise network or campus network) since we do not have global visibility on SPM malware propagation across networks. We assume that the attacker gets a foothold inside the local network through a single initially infected host. From the ‘patient zero’ victim, the attack can propagate and infect any other vulnerable machine in the subnet. We assume a homogeneous mixing model, meaning that every machine can contact all others. This is a valid assumption because in a subnet every machine is able to scan every other internal IP within the same subnet. We are assuming that none of the machines is immune to the exploited vulnerability at the beginning of the attack, thus, all of them may become infected during SPM propagation. Infectious machines become

recovered when the malware is successfully detected and an efficient recovery process removes it. We assume that these machines cannot be reinfected again.

III. SIIDR MODELLING AND ANALYSIS AS A SYSTEM OF ODES

In this section, we start by describing the important characteristics of the WannaCry propagation dynamic. We introduce the SIIDR model, and discuss the basic reproduction number and the stability of SIIDR disease-free equilibrium points.

A. SPM Modelling with SIIDR

The detailed analysis of the WannaCry traces [5] revealed the following characteristics:

- The time window Δt between two consecutive malicious attempts from the same infected IP has a heterogeneous distribution.
- The time interval Δt between the last attack from an infected IP and the end of the collected trace is large.

Based on the first observation, an infected dormant state I_D is included to capture the heterogeneous distribution of time windows between two malicious attack attempts. Therefore, an infected node can become dormant for some period of time and resume its malicious activity later. The second observation supports the presence of a Recovered state: once nodes recover, they will not become infectious or susceptible again. The transition diagram corresponding to the SIIDR model is illustrated in Figure 4. A susceptible node can become infected with rate β , and afterwards, it may either recover with rate μ , or move to the dormant state with rate γ_1 (where $\mu + \gamma_1 \leq 1$). From the dormant state, it may become actively infectious again with rate γ_2 .

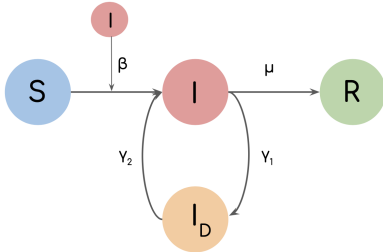


Figure 4: Transition diagram for one node n_i at some time step t corresponding to the SIIDR model.

The evolution of the system can be modeled through the system of ordinary differential equations (ODEs) as follows:

$$\frac{dS}{dt} = -\beta S \frac{I}{N} \quad (10)$$

$$\frac{dI}{dt} = \beta S \frac{I}{N} - \mu I - \gamma_1 I + \gamma_2 I_D \quad (11)$$

$$\frac{dI_D}{dt} = \gamma_1 I - \gamma_2 I_D \quad (12)$$

$$\frac{dR}{dt} = \mu I \quad (13)$$

with $N = S(t) + I(t) + I_D(t) + R(t)$, where the total size N is constant. It is important to stress how the system of ODEs assumes an homogeneous mixing in the host population.

B. SIIDR Equilibrium Points

While modeling SPM we are interested in equilibrium states when the number of infected individuals equals to 0 and does not change over time. Thus, we need to derive the constant solutions or equilibrium points [29] of the ODE system corresponding to SIIDR model.

Definition 1: An **equilibrium point** or **fixed point** of the system of ODEs $\dot{x} = f(X)$ is a solution E^* that does not change with time, i.e. $f(E^*) = 0$.

For the SIIDR model we can find the equilibrium points by solving the following system:

$$-\beta I \frac{S}{N} = 0 \quad (14)$$

$$\beta I \frac{S}{N} - \mu I - \gamma_1 I + \gamma_2 I_D = 0 \quad (15)$$

$$\gamma_1 I - \gamma_2 I_D = 0 \quad (16)$$

$$\mu I = 0 \quad (17)$$

given that $S + I + I_D + R = N$.

The system has the disease-free equilibrium points E^* when $I = I_D = 0$ and $S + R = N$. In case when $\mu = 0$ there exists endemic equilibrium point when $I \neq 0$ which is equal to $(0, I^*, \frac{\gamma_1 I^*}{\gamma_2}, 0)$. However, in this case the system becomes *SIID* without the opportunity to have R state.

C. The Basic Reproduction Number

The basic reproduction number R_0 is the number of secondary cases generated by a single infectious seed in a fully susceptible population [16]. It defines the epidemic threshold. The conditions that lead to a macroscopic outbreak. If R_0 has a value greater than 1, on average, infected individuals are able to sustain the spreading. If R_0 has a value smaller than one, on average, the disease will die out before any macroscopic outbreak.

A classic approach to compute R_0 is to linearize the ODEs using the fact that often at early times $S(0) \approx N$. We can sum equations 11 and 12 obtaining:

$$\frac{d(I + I_D)}{dt} = (\beta \frac{S}{N} - \mu) I \quad (18)$$

at early stages $S(0) \approx N$, hence we will have a growth in the number of the infected and infected dormant individuals only if $\beta - \mu > 0$. This leads to the condition $R_0 = \frac{\beta}{\mu}$.

Another method to derive the reproduction number is to use the next-generation matrix approach [3], [6], [7]. It takes into consideration the dynamic of infected individuals in compartment i , $i \in \{1, \dots, k\}$, where k is the number of compartments with infected individuals:

$$\frac{df_i(X)}{dt} = F_i(X) - V_i(X), \quad (19)$$

where $F_i(X)$ is the rate of appearance of new infections in compartment i by all other means, $V_i(X) = [V_i^-(X) - V_i^+(X)]$, $V_i^+(X)$ is the rate of transfer of individuals into compartment i and $V_i^-(X)$ represents the rate of transfer of individuals out of compartment.

If E^* is a disease-free equilibrium, then we can define a next-generation matrix:

$$G = FV^{-1}, \quad (20)$$

where

$$F = \frac{\partial F_i}{\partial x_j}(E^*) \quad (21)$$

$$V = \frac{\partial V_i}{\partial x_j}(E^*). \quad (22)$$

The reproduction number is the largest eigenvalue of the next-generation matrix G . In the case of SIIDR model, the G can be represented at one of the disease-free equilibrium points $DfE = (N, 0, 0, 0)$ as follows:

$$G = \begin{bmatrix} \beta & 0 \\ 0 & 0 \end{bmatrix} \begin{bmatrix} \mu + \gamma_1 & -\gamma_2 \\ -\gamma_1 & \gamma_2 \end{bmatrix}^{-1} = \begin{bmatrix} \frac{\beta}{\mu} & \frac{\beta}{\mu} \\ 0 & 0 \end{bmatrix} \quad (23)$$

thus $\det[\lambda I - G] = \lambda(\lambda - \frac{\beta}{\mu})$, and $R_0 = \frac{\beta}{\mu}$. We note how in general, the disease free equilibrium (DFE) might contain individuals already immune to the disease, i.e., $DfE = (N - R, 0, 0, R)$. This might be due to a second wave of infection caused by the reintroduction of the virus. In this more general case we have: $R_0 = \frac{\beta}{\mu} (1 - \frac{R}{N})$, where in parenthesis we have the fraction of the susceptible population.

D. Stability Analyses of SIIDR Equilibrium Points

The important characteristic of the equilibrium points is their stability [15]. It shows whether the system will be able to return to the equilibrium points after small perturbations. For example, in the case of SIIDR modeling, it can be the slightly increased number of initially infected nodes. Let us consider $\dot{x} = f(X)$ - system of ODEs, and suppose that $X = E^*$ is a fixed point of $f(X)$, that is, $f(E^*) = 0$.

Definition 2: E^* is **stable** if $\forall \epsilon > 0, \exists \delta > 0$ such that if an initial condition $X = X^0$ lies in the ball of radius δ around E^* then it exists $\forall t > 0$ and stays in the ball of radius ϵ .

Definition 3: We say that E^* is **locally asymptotically stable** if it is stable and the solutions $X = X^t$ with initial condition $X = X^0$ in the ball of radius δ converge to E^* as $t \rightarrow \infty$.

Definition 4: We say that E^* is **stable in the sense of Lyapunov** when there exists the continuously differentiable function $L(X)$ such that:

$$L(X) \geq 0, L(E^*) = 0 \quad (24)$$

$$\dot{L}(X) = \frac{d}{dt}L(X) = \sum_i \frac{dL}{dx_i} f_i(X) \leq 0, \dot{L}(E^*) = 0 \quad (25)$$

If $\dot{L}(X) < 0$ and $\dot{L}(X) = 0$ only when $X = E^*$, then E^* is **locally asymptotically stable**.

Theorem 1: If $R_0 \leq 1$ the disease-free equilibrium point E^* of SIIDR system of ODEs is stable in the sense of Lyapunov.

Proof: Let $L(X) = I + I_D$, L is the valid Lyapunov function as long as it is non-negative continuously differentiable scalar function which equals to 0 when $I = I_D = 0$. Time-derivative of L is the following:

$$\dot{L} = \frac{dL}{dt} = \beta S \frac{I}{N} - \mu I = I \left(\frac{\beta S}{\mu N} - 1 \right) = I(R_0 - 1) \quad (26)$$

Hence, we can conclude that $\dot{L} \leq 0$ when $R_0 \leq 1$ and $\dot{L}(E^*) = 0$. Therefore, E^* can be considered to be a disease-free equilibrium point stable in the sense of Lyapunov. \dot{L} is equal to 0 when $I = 0$, however, the X with $I = 0$ may not be equal to E^* , thus, we cannot consider E^* to be locally asymptotically stable. ■

IV. SIIDR MODELING

In this section, we explain the Akaike Information Criterion (AIC) technique used to select the model that fits the WannaCry malware best. We also demonstrate how we leverage the Sequential Monte-Carlo (SMC) approach to estimate the posterior distribution of SIIDR transition rates.

A. Model Selection

We use AIC to compare SIIDR to the most common epidemiological models and prove that it fits the real-world WannaCry traces best. AIC is calculated based on the number of free parameters used to fit the model and the maximum likelihood estimate of the model:

$$\text{AIC} = 2k - 2 \ln L \quad (27)$$

where k is the number of free parameters and L is the maximum likelihood. The first term introduces a penalty that increases with the number of parameters and thus discourages overfitting. The second term rewards the goodness of fit that is assessed by the likelihood function. For the likelihood function, we use the least squares estimation. This approach is valid when the residuals follow the normal distribution. Thus, the best model is the one with the lowest AIC. In the case of the least squares estimation, the AIC can be expressed as:

$$\text{AIC} = 2k + n \ln \hat{\sigma}^2, \text{ where} \quad (28)$$

$$\hat{\sigma}^2 = \frac{\sum_{t=1}^T \hat{\epsilon}_i}{T} \quad (29)$$

In Eq. 29, $\hat{\epsilon}_i$ are the estimated residuals:

$$\hat{\epsilon}_t = I_t^{sim} - I_t^{real} \quad (30)$$

with I_t^{sim} being the cumulative number of infected nodes from model simulations, and I_t^{real} the cumulative number of infected nodes from real-world observations, at time interval t .

To perform model selection, we use the method described in Algorithm 1. We start by creating a uniform grid of possible parameter values (lines 2-5). For each model and each set of parameter values $p = (\beta, \mu, \gamma_1, \gamma_2)$ we perform several stochastic experiments simulating the model dynamics (the run_stochastic_avg procedure). We use stochastic simulation over the direct integration of system of ODEs because they appear to be a good approximation of the propagation process only when the system is large. In the case of smaller systems stochastic fluctuations become more important. Therefore, we

are using them while performing model selection and parameter estimation. In our stochastic simulations, the transitions among compartments are implemented through chain binomial processes. At step t the number of entities in compartment X transiting to compartment Y is sampled from a binomial distribution $Pr^{Bin}(X(t), p_{X \rightarrow Y}(t))$, where $p_{X \rightarrow Y}(t)$ is the transition probability. If multiple transitions can happen from X (e.g., $X \rightarrow Y$, $X \rightarrow Z$), a multinomial distribution is used (e.g., $Pr^{Mult}(X(t), p_{X \rightarrow Y}(t), p_{X \rightarrow Z}(t))$). To account for the time component in equations 10-13, we divide the whole duration of the actual dynamics by d . Hence, each stochastic realization consists of a time series, where $S(t), I(t), I_D(t), R(t)$ represent the number of nodes in each state at time interval t during the simulation. The cumulative infection I_{sim} consists of the total number of nodes in states I, I_D , and R , and is also a time series across all time intervals dt . Next, we compute the AIC using equation 28 by comparing m simulated points to m (sampled) points from the actual dynamics. We select the minimum AIC score for each model, the best model is the one with the minimum AIC score overall.

Algorithm 1 SPM model selection

```

1: procedure MODEL_SELECTION
2:    $\beta \leftarrow 20$  equidistant values in (0,1)
3:    $\mu \leftarrow 20$  equidistant values in (0,1)
4:    $\gamma_1 \leftarrow 10$  equidistant values in (0,1)
5:    $\gamma_2 \leftarrow 10$  equidistant values in (0,1)
6:   for each model  $m = \{SI, SIS, SIR, SIIDR\}$  do
7:     for each set  $p = (\beta, \mu, \gamma_1, \gamma_2)$  do
8:        $S_i, I_i, I_{Di}, R_i = \text{run\_stochastic\_avg}(p, h)$ 
9:        $I_{sim} = I_i + I_{Di} + R_i$ 
10:       $aic = \text{AIC}(I_{sim}, I_{real})$ 
11:       $aic_{min}^m \leftarrow \min_i aic$ 
12:     $aic_{min} \leftarrow \min_m aic$ 
13:    pick  $M =$  model that correspond to  $aic_{min}$ 
14:  return  $M$ 

```

B. Posterior Distribution of Transition Rates

To find the best set of parameters for the SIIDR model we can approximate the posterior distribution of the parameters using Approximate Bayesian Computation (ABC) techniques [23]. These techniques are based on the Bayes rule for determining the posterior distribution of parameters given the data:

$$P(\theta|D) = \frac{P(D|\theta)P(\theta)}{p(D)} \propto p(D|\theta)p(\theta), \quad (31)$$

where $P(\theta)$ is the prior distribution of parameters that represents our belief about them and $P(D|\theta)$ is the likelihood function, the probability density function of the data given the parameters. Marginal likelihood of the data $P(D)$ does not depend on θ , and therefore the posterior distribution $P(\theta|D)$ is proportional to the numerator in 31.

ABC methods perform well when the likelihood function is unknown or is not feasible to estimate. The simplest version of ABC techniques ABC-rejection is illustrated in Algorithm 2. However, the algorithm is slow for the following reason: at each iteration, it proposes parameter values from the prior

distribution, which might not be part of the parameters' space. This results in a large distance between the actual and simulated models. Thus, if the threshold value ϵ is small, it becomes possible to result in an infinite number of iterations.

Algorithm 2 ABC-rejection algorithm

```

1: Sample  $\theta^*$  from the prior distribution  $P(\theta)$ .
2: Simulate SPM model  $D^*$  using  $\theta^*$ .
3: If  $\sum_{t=1}^T (D_t - D_t^*)^2 \leq \epsilon$  accept  $\theta^*$ , reject otherwise.
4: Repeat until  $N$  particles  $\theta^* = \{\theta_j^*, j = 1, \dots, N\}$  are accepted.

```

Alternatively, we can use the ABC-SMC [31] [21] approach where several generations of distributions are constructed by decreasing the threshold over time. At the first step (i.e., generation), a finite number of parameter sets (i.e., particles) is sampled from the prior distribution, and each intermediate distribution of particles is obtained as a weighted sample from the previous generation perturbed through the kernel $K(\theta|\theta^*)$. Common choices for the kernel are the uniform and multivariate normal distributions. A kernel with a large variance will prevent the algorithm from being stuck in the local modes, but will result in a huge number of particles being rejected, which is inefficient. Therefore, we use the multivariate normal distribution, where the covariance matrix is calculated considering M nearest neighbors of the particles [9]. The ABC-SMC-MNN algorithm is illustrated in Algorithm 3.

Algorithm 3 SIIDR parameters estimation

Require: G - number of generations, N - number of particles, M - number of nearest neighbors, $\epsilon_1 > \epsilon_2 > \epsilon_3 > \dots > \epsilon_G$ - sequence of decreasing tolerance values for each generation of the particles

```

1: Set  $g = 0$ 
2: Set  $j = 0$ 
3: If  $g = 0$ , sample particle  $\theta^{**}$  from prior distribution  $P(\theta)$ . Otherwise, sample  $\theta^*$  from the previous generation of particles  $\{\theta_{g-1}^*\}$  with weights  $\{w_{g-1}\}$  and perturb to obtain  $\theta^{**} \sim K(\theta|\theta^*)$ 
4: Generate  $n$  model simulations  $D_l^{**}$  using  $\theta^*$  and calculate  $\hat{P}(D|D^{**}) = 1/n \sum_{l=1}^n (d(D, D_l^{**}) < \epsilon_g)$ 
5: If  $\hat{P}(D|D^{**}) = 0$  return to step 4
6: Set  $\theta_g^j$  and calculate weights for the particle:

```

$$w_g^j = \begin{cases} \hat{P}(D|D^{**})P(\theta^{**}), & g = 1 \\ \frac{\hat{P}(D|D^{**})P(\theta^{**})}{\sum_{l=1}^N w_{g-1}^l K(\theta_g^j|\theta_{g-1}^l)}, & g > 1 \end{cases}$$

```

7: If  $j < N$  increment  $j$  and go to step 4
8: Normalize weights:  $\sum_{j=1}^N w_g^j = 1$ 
9: If  $g < G$  increment  $g$  and go to step 3

```

V. EXPERIMENTAL RESULTS

In this section we describe the WannaCry malware traces and show the results of the reconstruction of WannaCry dynamics from Zeek [1] communication logs. Additionally, we present the results from model selection to confirm that SIIDR fits WannaCry traces best. Moreover, we illustrate the mean values from the posterior distribution of SIIDR parameters.

Finally, we show the behavior of SPM with respect to the basic reproduction number R_0 .

A. WannaCry Malware Traces

We obtained realistic WannaCry attack traces by running the malware in a controlled virtual environment consisting of 51 virtual machines, configured with a version of Windows vulnerable to the EternalBlue SMB exploit. The external traffic generated by the VMs was blocked to isolate the environment and prevent external malware spread. The infection started from an initial victim IP, and then the attack propagated through the network as the infected IPs began to scan other IPs. In these experiments, WannaCry varied the number of threads used for scanning, which were set to 1, 4 or 8, and the time interval between scans, which was set to 500ms, 1s, 5s, 10s or 20s. Using the combination of these two parameters resulted in 15 WannaCry traces. While running WannaCry with this setup, the log traces were collected with the help of the open source Zeek network monitoring tool.

B. WannaCry Reconstruction

To reconstruct the WannaCry dynamics we are using Zeek communication logs where we consider only communication between internal IPs. Since WannaCry attempts to exploit the SMB vulnerability, we label as malicious all the attempts of connections on destination port 445. The first attempt to establish the malicious connection is considered to be the start of the epidemics, and the end corresponds to the last communication event in the network. Each IP trying to establish a malicious connection for the first time at time t is considered infected at time t . The cumulative number of infected IPs through time represents the curve of the WannaCry epidemics.

C. WannaCry dynamics

We show the dynamics of WannaCry variants characterized by different numbers of scanning threads and time between scans in Figure 5. These dynamics represent the cumulative number of infected nodes during the epidemic time. The trace which corresponds to 1 thread and 20s sleeping time wc_1_20s has unusual behavior in the dynamics. It has a very small number of infected nodes until the end of the attack, when the infections rapidly increase to the 7 infected nodes at once. For all other WannaCry variants we observe that the attack reaches the maximum number of infected nodes quickly and is not able to infect any other nodes for a large time window before the end of the epidemic. These graphs confirm the fact that after an IP enters a recovered state it no longer has an opportunity to get back to susceptible or infected nodes. For modeling and parameter estimation experiments we exclude the time windows after which the number of infections does not change. Additionally, we present the number of contacted and infected IPs in Table II. Interestingly, the overall percentage of infected nodes is small (around 25% on average) for all variants, which indicates the fact that the attack propagates slowly through the network.

D. Model Selection

We select the model that fits WannaCry traces best among several representative compartmental epidemiological models:

SI, SIS, SIR and SIIDR. We perform model selection for all WannaCry traces. For these purposes, we use AIC which is calculated based on the maximum likelihood estimate and the number of free model parameters. The lower AIC score corresponds to the best model. We run the experiments on a uniform grid of model parameter values between 0 and 1. We select the lowest AIC score for each WannaCry trace and each compartmental model. The results are illustrated in Table III. The SIIDR model has the lowest AIC score for all traces except for wc_1_20s . For instance, the AIC score associated with the SI model for wc_8_5s WannaCry trace is equal to 149, the SIS model score is 104, the SIR model score is -35, whereas for the SIIDR model the AIC is the lowest and has the value of -121, which is much lower than others. This trend is valid for all other WannaCry traces except for wc_1_20s which has very high AIC scores for all models. This variant is an outlier and none of the models is able to fit the wc_1_20s trace. Therefore, we can conclude that, among the four epidemiological models, the SIIDR model fits the WannaCry attack traces best.

For each compartmental model and each WannaCry trace, we plot the reconstruction curve of the number of infected nodes using the parameters corresponding to the lowest AIC score along with the true dynamics of infected nodes. The results are shown in Figure 6. In the case of the SI and SIS model, the orange line representing the simulated dynamics of the number of infected nodes is far from the blue one, which illustrates the true dynamic for all malware traces. In the case of the SIR model the numbers of simulated infections are closer to the real ones, however, the orange and blue curves are the closest when simulating WannaCry with the SIIDR model. These results also confirm the fact that SIIDR is the best model to fit the WannaCry traces.

E. Parameter estimation

We approximated the posterior distribution of SIIDR transition rates using the ABC-SMC-MNN technique. The mean values of the posterior distribution of SIIDR transition rates (β , μ , γ_1 , γ_2) are represented in Table IV. The parameter dt is the simulation timestamp, which is calculated as: $dt = (t_N - t_0)/T$, where t_N is the last timestamp, t_0 is the first timestamp, and T is the number of timestamps in WannaCry traces. dt differs by variant due to the different propagation speeds. The attack transmission probability $\tilde{\beta}$ is related to attack transmission rate β as follows: $\beta = \tilde{\beta} \langle k \rangle_t$ where $\langle k \rangle_t$ is the average contact rate per unit time. In the WannaCry traces we have one communication or contact per dt , hence, the transmission probability $\tilde{\beta}$ over a contact-link also equals β .

Based on estimated values of transition rates we calculated the basic reproduction number R_0 for all WannaCry traces. We also calculate the SPM propagation speed for all WannaCry traces as the average number of new infections per 100 seconds. The results are illustrated in Figure 7, where higher values of SPM propagation speed correspond to higher basic reproduction number R_0 .

The mean values of the parameters' posterior distribution can be further used to simulate SPM with the SIIDR model. This provides an opportunity to create synthetic, but realistic, WannaCry scenarios and evaluate whether existing defenses

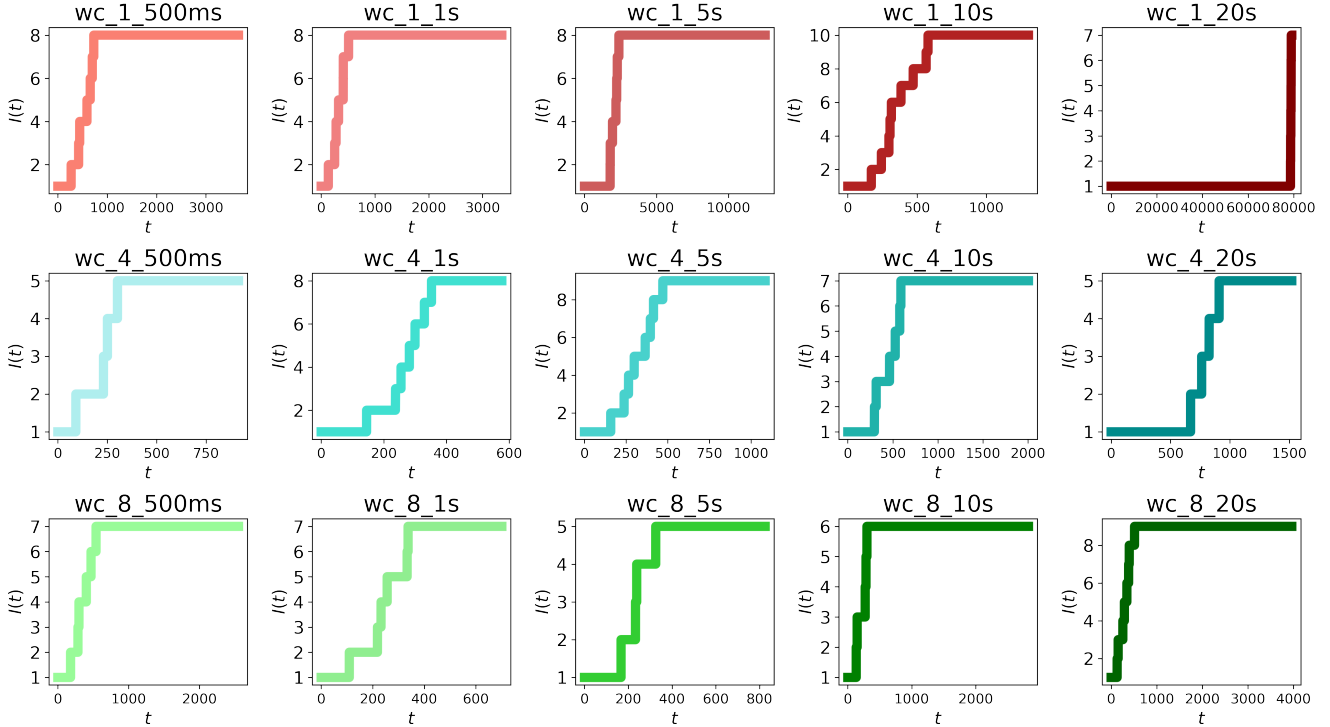


Figure 5: The cumulative number of the infected nodes $I(t)$ (counting all nodes in states I , I_D and R) at each time point t of WannaCry propagation for different variants of WannaCry. Each WannaCry variant is identified by two parameters: the number of threads used for scanning and the time interval between scans (i.e., wc_1_500ms uses 1 thread to scan every 500 ms).

WannaCry Variant	# Contacted IPs	# Infected IPs	Percentage of Infected IPs
wc_1_500s	37	8	0.22
wc_1_1s	37	8	0.22
wc_1_5s	37	8	0.22
wc_1_10s	34	10	0.29
wc_1_20s	35	7	0.20
wc_4_500ms	34	5	0.15
wc_4_1s	35	8	0.23
wc_4_5s	36	9	0.25
wc_4_10s	35	7	0.20
wc_4_20s	35	5	0.14
wc_8_500ms	35	7	0.20
wc_8_1s	35	7	0.20
wc_8_5s	35	5	0.14
wc_8_10s	36	6	0.17
wc_8_20s	35	9	0.26

Table II: Number of contacted and Infected IP addresses from communication data for WannaCry modeling.

are successful in preventing and stopping the malware from propagation in the networks. However, we notice that some of the WannaCry traces operate affect only a small numbers of nodes. For example, the wc_8_5s trace has only 4 infected nodes at the end of the trace which constitutes 14% of all nodes. Consequently, ABC-SMC-MNN is expected to perform worse in the estimation of transition rates for such traces. Thus, parameters estimated from the traces with higher numbers are more reliable.

VI. RELATED WORK

A number of works propose to capture the possible behavior of SPM with epidemic models. Mishra et al. [24] introduce the SEIQRS model for viruses and study the effect

of the quarantined compartment on the number of recovered nodes. In their paper, the authors focus on the analyses of the threshold that determines the outcome of the disease. Mishra et al. [25] introduce the SEIS-V model for viruses with a vaccinated state. Mishra et al. [26] propose the SEIRS model and investigate the malicious objects' free equilibrium stating the stability of the results in terms of the threshold parameter. Toutonji et al. [33] propose a VEISV (Vulnerable-Exposed-Infectious-Secured-Vulnerable) model and use the reproduction rate to derive global and local stability. With the help of simulation, they show the positive impact of increasing security countermeasures in the vulnerable state on worm-exposed and infectious propagation waves. Guillen et al. [13] introduce a SCIRAS (Susceptible-Carrier-Infectious-

WannaCry variant	SI	SIS	SIR	SIIDR
wc_1_500ms	583	143	114	-126
wc_1_1s	431	188	145	-127
wc_1_5s	683	163	143	72
wc_1_10s	462	197	53	-92
wc_1_20s	704	559	696	700
wc_4_500ms	277	76	-45	-166
wc_4_1s	222	160	107	-55
wc_4_5s	412	186	158	-46

WannaCry variant	SI	SIS	SIR	SIIDR
wc_4_10s	513	94	-36	-145
wc_4_20s	606	76	11	-117
wc_8_500ms	375	101	18	-147
wc_8_1s	178	91	51	-116
wc_8_5s	149	104	-35	-121
wc_8_10s	253	74	-90	-118
wc_8_20s	387	164	173	-89

Table III: AIC scores for each of the SPM models for different WannaCry variants. The lower is the better.

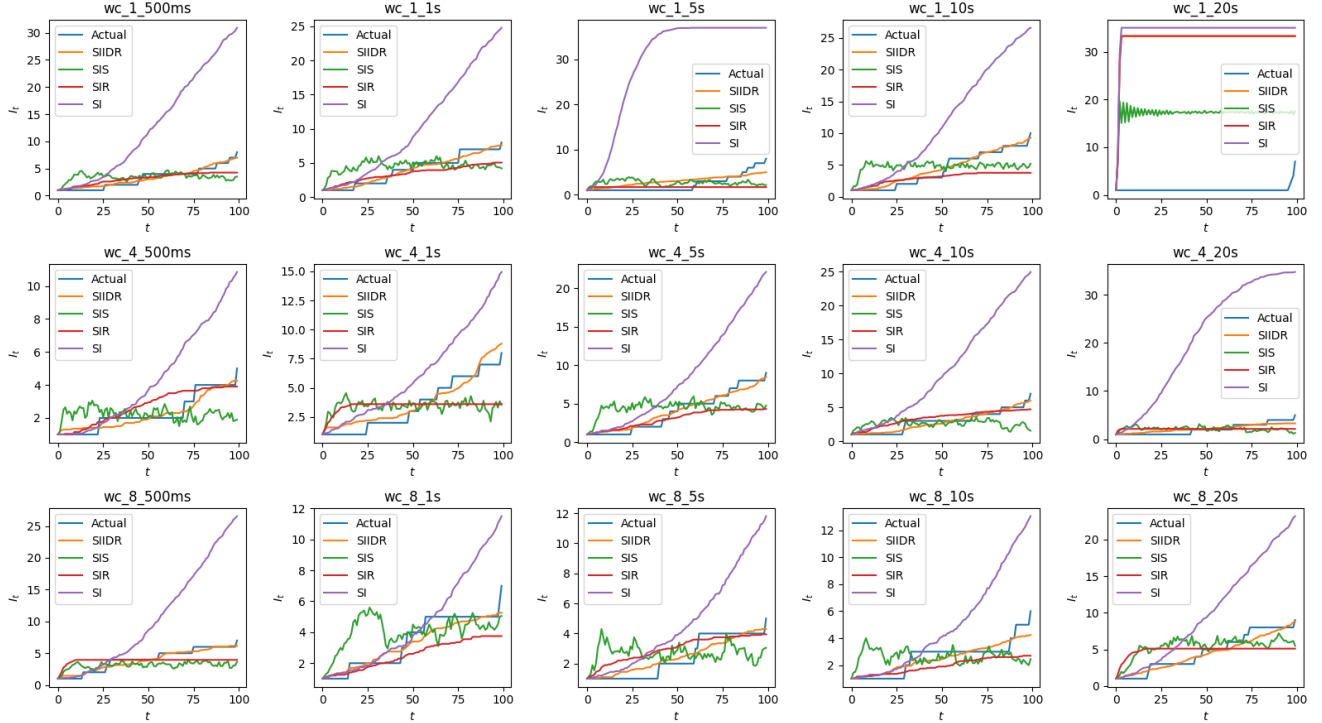


Figure 6: Model fitting for different WannaCry variants.

WannaCry variant	β	μ	γ_1	γ_2	dt
wc_1_500ms	0.10	0.06	0.76	0.04	0.09
wc_1_1s	0.11	0.07	0.71	0.07	0.06
wc_1_5s	0.37	0.52	0.27	0.44	0.16
wc_1_10s	0.12	0.06	0.75	0.05	0.09
wc_1_20s	0.22	0.54	0.24	0.46	0.99
wc_4_500ms	0.39	0.54	0.27	0.45	0.05
wc_4_1s	0.14	0.07	0.75	0.08	0.05
wc_4_5s	0.12	0.07	0.76	0.07	0.07
wc_4_10s	0.39	0.53	0.27	0.47	0.10
wc_4_20s	0.37	0.53	0.28	0.47	0.14
wc_8_500ms	0.10	0.09	0.72	0.11	0.03
wc_8_1s	0.17	0.15	0.66	0.12	0.03
wc_8_5s	0.42	0.54	0.27	0.50	0.07
wc_8_10s	0.38	0.54	0.26	0.47	0.06
wc_8_20s	0.13	0.09	0.74	0.08	0.07

Table IV: Mean values from posterior distribution of SIIDR parameters estimated with the ABC-SMC-MNN method.

Recovered-Attacked-Susceptible) model. Authors study the local and global stability of its equilibrium points and compute the basic reproductive number. Ojha et al. [27] develop a new SEIQRV (Susceptible-Exposed-Infected -Quarantined-Recovered-Vaccinated) model to capture the behavior of SPM.

In their work, authors obtain the equilibrium points of the proposed model, analyze the system stability under different conditions, and verify theoretically through simulation results. Zheng et al. [40] introduce the SLBQR (Susceptible-Latent-Breaking out-Quarantined-Recovered) model considering vac-

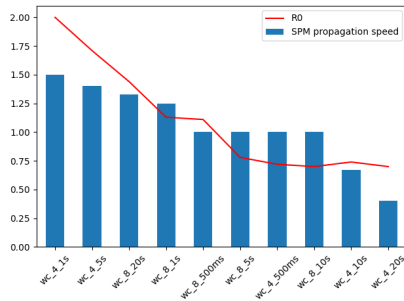


Figure 7: The basic reproduction number R_0 calculated by using estimated values of transition rates compared to the speed of SPM propagation. Higher propagation speed corresponds to higher R_0 . We exclude the results for the wc_1* traces.

ination strategies with temporary immunity as well as quarantined strategies. The authors study the stability of the model, investigate a strategy, based on quarantines, to suppress the spread of the virus and discuss the effect of the vaccination on permanent immunity. In order to verify their findings, the authors simulate the model exploring a range of temporary immune times and quarantine rates.

Another direction of research focuses on dynamical systems for SPM modeling. In their work, Guillen et al. [14] study the SEIRS model and use a modified incidence rate in it. Additionally, the equilibrium points are computed and their local and global stability analyses are studied. Finally, the authors derive the explicit expression of the basic reproductive number and obtain the corresponding efficient control measures. Martinez et al. [20] introduce a dynamic version of the SEIRS version. The authors look at the performance of the model with different sets of parameters, propose optimal values, and discuss its applicability to model real-world malware. Gan et al. [11] propose a dynamical SIP (Susceptible - Infected - Protected) model, find an equilibrium point, and discuss its local and global stability. Additionally, the authors perform the numerical simulations of the model to demonstrate the dependency on parameter values. Yao et al. [39] present a time-delayed worm propagation model with variable infection rate. They analyze the stability of equilibrium and the threshold of Hopf bifurcation. The authors carry out the numerical analysis and simulation of the model.

Some of the authors explore the idea of the presence of different types of devices in the network and consider it while modeling the SPM behavior with ODE. For instance, Guillen et al. [12] introduce the model for SPM that considers the special class of carrier devices whose operative systems are not targeted by the malware (for example, iOS devices for Android malware) by introducing a new compartment. The authors analyze the efficient control measures by studying the basic reproductive number. Zhu et al. [41] discuss the model that takes into consideration the fact that viruses can infect not only computers but also many kinds of external removable devices. Thus, internal devices can be in Susceptible, Infected, and Recovered states, while removable devices can be in Susceptible and Infected states.

None of these works mentioned perform model fitting to

real-world malware scenarios, but only consider theoretical analyses of the proposed models. The closest to our work is Levy et al. [19], where the authors fit SPM with a SIR model and study how the introduction of signatures affects the spread of malware. They show how early vaccination can prevent the spread of SPM.

VII. CONCLUSIONS

In our work, we performed a comprehensive analysis of a new compartmental model SIIDR that captures the behavior of self-propagating malware. Indeed, we showed that it fits real-world WannaCry traces much better than existing compartmental models such as SI, SIS, and SIR previously studied in the literature. Additionally, we estimated the posterior distribution of the model's parameters for real attack traces and showed how they characterize the WannaCry behavior. We also analytically derived the conditions when SPM is expected to become an epidemic in well-mixed populations and discussed the stability of model's equilibrium points. Our work can have an impact to model the propagation of SPM, simulate real attacks on networks, and evaluate defensive techniques.

ACKNOWLEDGMENT

We acknowledge Jason Hiser and Jack W. Davidson from University of Virginia for providing us access to the WannaCry attack traces.

This research was sponsored by the U.S. Army Combat Capabilities Development Command Army Research Laboratory under Cooperative Agreement Number W911NF-13-2-0045 (ARL Cyber Security CRA). The views and conclusions contained in this document are those of the authors and should not be interpreted as representing the official policies, either expressed or implied, of the Combat Capabilities Development Command Army Research Laboratory or the U.S. Government. The U.S. Government is authorized to reproduce and distribute reprints for Government purposes notwithstanding any copyright notation here on.

REFERENCES

- [1] "Zeek," <https://docs.zeek.org/en/master/script-reference/log-files.html>, accessed: 2022-07-11.
- [2] H. Akaike, "A new look at the statistical model identification," *IEEE Transactions on Automatic Control*, vol. 19, no. 6, pp. 716–723, 1974.
- [3] J. C. Blackwood and L. M. Childs, "An introduction to compartmental modeling for the budding infectious disease modeler," *Letters in Biomathematics*, 2018.
- [4] F. Brauer, "Compartmental models in epidemiology," in *Mathematical epidemiology*. Springer, 2008, pp. 19–79.
- [5] A. Chernikova, N. Gozzi, S. Boboila, P. Angadi, J. Loughner, M. Wilden, N. Perra, T. Eliassi-Rad, and A. Oprea, "Cyber network resilience against self-propagating malware attacks," in *Proceedings 27th European Symposium on Research in Computer Security (ESORICS) 2022*.
- [6] O. Diekmann, J. Heesterbeek, and M. G. Roberts, "The construction of next-generation matrices for compartmental epidemic models," *Journal of the royal society interface*, vol. 7, no. 47, pp. 873–885, 2010.
- [7] O. Diekmann, J. A. P. Heesterbeek, and J. A. Metz, "On the definition and the computation of the basic reproduction ratio r_0 in models for infectious diseases in heterogeneous populations," *Journal of mathematical biology*, vol. 28, no. 4, pp. 365–382, 1990.

- [8] K. Dietz, "The estimation of the basic reproduction number for infectious diseases," *Statistical methods in medical research*, vol. 2, no. 1, pp. 23–41, 1993.
- [9] S. Filippi, C. P. Barnes, J. Cornebise, and M. P. Stumpf, "On optimality of kernels for approximate bayesian computation using sequential monte carlo," *Statistical applications in genetics and molecular biology*, vol. 12, no. 1, pp. 87–107, 2013.
- [10] C. Fraser, C. A. Donnelly, S. Cauchemez, W. P. Hanage, M. D. Van Kerkhove, T. D. Hollingsworth, J. Griffin, R. F. Baggaley, H. E. Jenkins, E. J. Lyons *et al.*, "Pandemic potential of a strain of influenza a (h1n1): early findings," *science*, vol. 324, no. 5934, pp. 1557–1561, 2009.
- [11] C. Gan, Q. Feng, X. Zhang, Z. Zhang, and Q. Zhu, "Dynamical propagation model of malware for cloud computing security," *IEEE Access*, vol. 8, pp. 20 325–20 333, 2020.
- [12] J. H. Guillén and A. M. del Rey, "Modeling malware propagation using a carrier compartment," *Communications in Nonlinear Science and Numerical Simulation*, vol. 56, pp. 217–226, 2018.
- [13] J. H. Guillén, A. M. Del Rey, and R. Casado-Vara, "Security countermeasures of a sciras model for advanced malware propagation," *IEEE Access*, vol. 7, pp. 135 472–135 478, 2019.
- [14] J. H. Guillén, A. M. Del Rey, and L. H. Encinas, "Study of the stability of a seirs model for computer worm propagation," *Physica A: Statistical Mechanics and its Applications*, vol. 479, pp. 411–421, 2017.
- [15] M. Hirsch and S. Smale, *Differential equations, dynamical systems, and linear algebra*. Academic Press, 1974.
- [16] M. J. Keeling and P. Rohani, *Modeling infectious diseases in humans and animals*. Princeton university press, 2011.
- [17] J. O. Kephart and S. R. White, "Measuring and modeling computer virus prevalence," in *Proceedings 1993 IEEE Computer Society Symposium on Research in Security and Privacy*. IEEE, 1993, pp. 2–15.
- [18] L. T. Le, T. Eliassi-Rad, and H. Tong, "MET: A fast algorithm for minimizing propagation in large graphs with small eigen-gaps," in *SDM*, 2015, pp. 694–702.
- [19] N. Levy, A. Rubin, and E. Yom-Tov, "Modeling infection methods of computer malware in the presence of vaccinations using epidemiological models: an analysis of real-world data," *International Journal of Data Science and Analytics*, vol. 10, no. 4, pp. 349–358, 2020.
- [20] I. Martínez Martínez, A. Florián Quitián, D. Díaz-López, P. Nespoli, and F. Gómez Mármol, "Malseirs: Forecasting malware spread based on compartmental models in epidemiology," *Complexity*, vol. 2021, 2021.
- [21] T. J. McKinley, I. Vernon, I. Andrianakis, N. McCreesh, J. E. Oakley, R. N. Nsubuga, M. Goldstein, and R. G. White, "Approximate bayesian computation and simulation-based inference for complex stochastic epidemic models," *Statistical science*, vol. 33, no. 1, pp. 4–18, 2018.
- [22] Mike Azzara, "What is wannacry ransomware and how does it work?" <https://www.mimecast.com/blog/all-you-need-to-know-about-wannacry-ransomware/>, 2021.
- [23] A. Minter and R. Retkute, "Approximate bayesian computation for infectious disease modelling," *Epidemics*, vol. 29, p. 100368, 2019.
- [24] B. K. Mishra and N. Jha, "Seiqrs model for the transmission of malicious objects in computer network," *Applied Mathematical Modelling*, vol. 34, no. 3, pp. 710–715, 2010.
- [25] B. K. Mishra and S. K. Pandey, "Dynamic model of worm propagation in computer network," *Applied mathematical modelling*, vol. 38, no. 7-8, pp. 2173–2179, 2014.
- [26] B. K. Mishra and D. K. Saini, "Seirs epidemic model with delay for transmission of malicious objects in computer network," *Applied mathematics and computation*, vol. 188, no. 2, pp. 1476–1482, 2007.
- [27] R. P. Ojha, P. K. Srivastava, G. Sanyal, and N. Gupta, "Improved model for the stability analysis of wireless sensor network against malware attacks," *Wireless Personal Communications*, vol. 116, no. 3, pp. 2525–2548, 2021.
- [28] T. Ongun, O. Spohngellert, B. A. Miller, S. Boboila, A. Oprea, T. Eliassi-Rad, J. Hiser, A. Nottingham, J. W. Davidson, and M. Veer-araghavan, "PORTFILER: Port-Level Network Profiling for Self-Propagating Malware Detection," in *CNS*. IEEE, 2021, pp. 182–190.
- [29] L. Perko, *Differential Equations and Dynamical Systems*. Springer Science & Business Media, 2013, vol. 7.
- [30] H. Tong, B. A. Prakash, T. Eliassi-Rad, M. Faloutsos, and C. Faloutsos, "Gelling, and melting, large graphs by edge manipulation," in *CIKM*, 2012, pp. 245–254.
- [31] T. Toni, D. Welch, N. Strelkowa, A. Ipsen, and M. P. Stumpf, "Approximate bayesian computation scheme for parameter inference and model selection in dynamical systems," *Journal of the Royal Society Interface*, vol. 6, no. 31, pp. 187–202, 2009.
- [32] L. Torres, K. Chan, H. Tong, and T. Eliassi-Rad, "Nonbacktracking eigenvalues under node removal: X-centrality and targeted immunization," *SIAM Journal on Mathematics of Data Science*, vol. 3, pp. 656–675, 01 2021.
- [33] O. A. Toutonji, S.-M. Yoo, and M. Park, "Stability analysis of veisv propagation modeling for network worm attack," *Applied Mathematical Modelling*, vol. 36, no. 6, pp. 2751–2761, 2012.
- [34] P. Van den Driessche and J. Watmough, "Further notes on the basic reproduction number," *Mathematical epidemiology*, pp. 159–178, 2008.
- [35] A. Vespignani, "Modelling dynamical processes in complex socio-technical systems," *Nature Physics*, vol. 8, no. 1, pp. 32–39, 2012.
- [36] Wikipedia, "Colonial pipeline ransomware attack," https://en.wikipedia.org/wiki/Colonial_Pipeline_ransomware_attack, Accessed April 2022.
- [37] Wikipedia contributors, "Petya and notpetya — Wikipedia, the free encyclopedia," 2022, [Online; accessed 22-June-2022]. [Online]. Available: https://en.wikipedia.org/w/index.php?title=Petya_and_NotPetya&oldid=1090033619
- [38] —, "Wannacry ransomware attack — Wikipedia, the free encyclopedia," 2022, [Online; accessed 7-May-2022]. [Online]. Available: https://en.wikipedia.org/w/index.php?title=WannaCry_ransomware_attack&oldid=1086034703
- [39] Y. Yao, Q. Fu, W. Yang, Y. Wang, and C. Sheng, "An epidemic model of computer worms with time delay and variable infection rate," *Security and Communication Networks*, vol. 2018, 2018.
- [40] Y. Zheng, J. Zhu, and C. Lai, "A seiqr model considering the effects of different quarantined rates on worm propagation in mobile internet," *Mathematical Problems in Engineering*, vol. 2020, 2020.
- [41] Q. Zhu, X. Yang, and J. Ren, "Modeling and analysis of the spread of computer virus," *Communications in Nonlinear Science and Numerical Simulation*, vol. 17, no. 12, pp. 5117–5124, 2012.